

---

# Constant Memory Attentive Neural Processes

---

**Leo Feng**

Mila – Université de Montréal & Borealis AI  
leo.feng@mila.quebec

**Frederick Tung**

Borealis AI  
frederick.tung@borealisai.com

**Hossein Hajimirsadeghi**

Borealis AI  
hossein.hajimirsadeghi@borealisai.com

**Yoshua Bengio**

Mila – Université de Montréal  
yoshua.bengio@mila.quebec

**Mohamed Osama Ahmed**

Borealis AI  
mohamed.o.ahmed@borealisai.com

## Abstract

Neural Processes (NPs) are efficient methods for estimating predictive uncertainties. NPs comprise of a conditioning phase where a context dataset is encoded, a querying phase where the model makes predictions using the context dataset encoding, and an updating phase where the model updates its encoding with newly received datapoints. However, state-of-the-art methods require additional memory which scales linearly or quadratically with the size of the dataset, limiting their applications, particularly in low-resource settings. In this work, we propose Constant Memory Attentive Neural Processes (CMANPs), an NP variant which only requires **constant** memory for the conditioning, querying, and updating phases. In building CMANPs, we propose Constant Memory Attention Block (CMAB), a novel general-purpose attention block that can compute its output in constant memory and perform updates in constant computation. Empirically, we show CMANPs achieve state-of-the-art results on meta-regression and image completion tasks while being (1) significantly more memory efficient than prior methods and (2) more scalable to harder settings.

## 1 Introduction

NPs are popular meta-learning methods for modelling uncertainty due to being more computationally efficient than traditional methods such as ensembles (Lakshminarayanan et al., 2017) or MC-Dropout (Gal and Ghahramani, 2016) which require training of a neural network. Rather than having to train on the dataset, NPs, in a *conditioning step*, compute embeddings representative of the context (training) dataset. NP’s efficiency makes them particularly useful in regimes with limited resources (e.g., compute or memory) or data streams (e.g., contextual multi-armed bandit, active learning, or bayesian optimization) where the amount of data increases frequently.

After conditioning, in the *querying step*, NPs make predictions on target datapoints using the pre-computed dataset embeddings. Recently, attention-based NP methods Transformer Neural Processes (TNPs) (Nguyen and Grover, 2022) and Latent Bottlenecked Attentive Neural Processes (LBANPs) (Feng et al., 2023) have achieved vastly superior results in comparison with prior NP works. The state-of-the-art method TNPs (Nguyen and Grover, 2022) utilise transformer layers whose computation scales quadratically  $O((N + M)^2)$  with respect to the number of context ( $N$ ) and target data points ( $M$ ). Improving on TNPs, LBANPs (Feng et al., 2023) utilise a Perceiver-like

attention mechanism (Jaegle et al., 2021) requiring  $O(NL)$  computation in the conditioning step where  $L$  is a hyperparameter that scales according to the difficulty of the task. Although subquadratic alternatives like LBNPs have been proposed for settings with large context dataset sizes such as image completion and genetic imputation (Rastogi et al., 2023), these current state-of-the-art NP methods have limited effectiveness as (1) the model’s memory requirement when performing the conditioning step is still highly dependent on the size of the context dataset, limiting its scalability, and (2) in the *update step* where new datapoints are added to the context dataset, the existing models require re-computing the conditioning step again on the updated **full** context dataset, requiring the storing of the full context dataset to update the model. These issues render these methods inapplicable in low compute domains (e.g., IoT devices, mobile phones and other battery-powered devices) or in data stream settings where often the dataset cannot be stored.

In this work, we propose Constant Memory Attentive Neural Processes (CMANPs), which only require **constant** memory complexity for conditioning, querying, and updating. To this end, we develop a novel attention block called the Constant Memory Attention Block (CMAB) which allows (1) computing its output in constant memory regardless of the number of inputs and (2) performing updates to the attention block’s input in constant computation. Furthermore, CMABs does not require storing the input to update its output; as a result, unlike prior attention-based NP methods, CMANPs also do not require storing of the context dataset to perform updates when deployed. Leveraging the efficient updates property, we further introduce an Autoregressive Not-Diagonal variant, namely, CMANP-AND. In the experiments, CMANPs achieve state-of-the-art results on meta-regression and image completion tasks while being more scalable and memory efficient than prior methods such as TNPs and LBNPs.

## 2 Background

### 2.1 Meta-learning for Predictive Uncertainty Estimation

In meta-learning for predictive uncertainty estimation, models are trained on a distribution of tasks  $\Omega(\mathcal{T})$  to model a probabilistic predictive distribution. A task  $\mathcal{T}$  is a tuple  $(\mathcal{X}, \mathcal{Y}, \mathcal{L}, q)$  where  $\mathcal{X}, \mathcal{Y}$  are the input and output space respectively,  $\mathcal{L}$  is the task-specific loss function, and  $q(x, y)$  is the task-specific distribution over data points. During each meta-training iteration,  $B_T$  tasks  $\mathbf{T} = \{\mathcal{T}_i\}_{i=1}^{B_T}$  are sampled from the task distribution  $\Omega(\mathcal{T})$ . For each task  $\mathcal{T}_i \in \mathbf{T}$ , a context dataset  $\mathcal{D}_i^{\text{context}} = \{(x, y)^{i,j}\}_{j=1}^N$  and a target dataset  $\mathcal{D}_i^{\text{target}} = \{(x, y)^{i,j}\}_{j=1}^M$  are sampled from the task-specific data point distribution  $q_{\mathcal{T}_i}$ .  $N$  is a fixed number of context datapoints and  $M$  is a fixed number of target datapoints. The model is adapted using the context dataset. Afterwards, the target dataset is used to evaluate the effectiveness of the adaptation and adjust the adaptation rule accordingly.

### 2.2 Neural Processes

Neural Processes (NPs) are meta-learned models that define a family of conditional distributions. Specifically, NPs condition on an arbitrary amount of context datapoints (labelled datapoints) and make predictions for a batch of target datapoints, while preserving invariance in the ordering of the context dataset. Prior works have modelled NPs as follows:

$$p(y|x, \mathcal{D}_{\text{context}}) := p(y|x, r_C) \quad (1)$$

where  $r_C := \text{Agg}(\mathcal{D}_{\text{context}})$  such that  $\text{Agg}$  is a deterministic function that aggregates the context dataset  $\mathcal{D}_{\text{context}}$  into a finite representation. NPs are trained to maximise the likelihood of the target dataset given the context dataset. Conditional Neural Processes (CNPs) (Garnelo et al., 2018a) proposed an aggregator based on deep sets (Zaheer et al., 2017) whereas other works such as Conditional Attentive Neural Processes (CANPs) (Kim et al., 2019) and Latent Bottlenecked Attentive Neural Processes (LBNPs) (Feng et al., 2023) proposed aggregators based on attention.

NPs consist of three phases: conditioning, querying, and updating. In the conditioning phase, the model computes embeddings of the context dataset  $r_C$ , i.e.,  $r_C := \text{Agg}(\mathcal{D}_{\text{context}})$ . During the querying phase, the model makes predictions for batches of target datapoints given the embeddings  $r_C$ . In the updating phase, the model receives new datapoints  $\mathcal{D}_{\text{update}}$ , and a new embedding  $r'_C$  is computed, i.e.,  $r'_C := \text{Agg}(\mathcal{D}_{\text{context}} \cup \mathcal{D}_{\text{update}})$ .

### 3 Methodology

In this section, we introduce the Constant Memory Attention Block (CMAB) which allows for computing its output in constant memory and performing updates to its input in constant computation. Building on CMAB, we construct Constant Memory Attentive Neural Processes (CMANPs). Leveraging the efficient updates capabilities of CMABs and CMANPs, we further introduce CMANP-AND (Autoregressive Not-Diagonal) which only requires constant memory in contrast to the quadratic memory required by prior Not-Diagonal NP variants, allowing for greater scalability.

#### 3.1 Constant Memory Attention Block (CMAB)

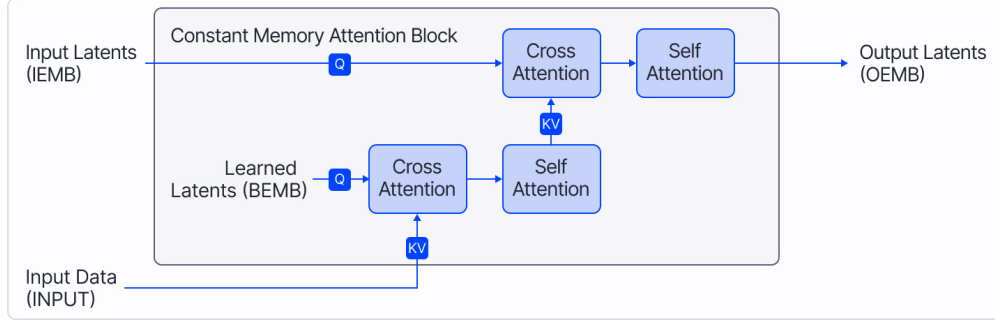


Figure 1: Constant Memory Attention Block (CMAB).

The Constant Memory Attention Block (Figure 1) takes as input the input data  $INPUT$  and a set of  $L_I$  input latent vectors  $IEMB$  and outputs a set of  $L_I$  output latent vectors  $OEMB$ . The objective of the block is to encode the information of the input data into a fixed sized representation similar to the objective of iterative attention (Jaegle et al., 2021). However, unlike prior works, our proposed attention mechanism crucially allows for applying updates to the input data in constant computation per datapoint. When stacking CMABs, the output latent vectors of the previous CMAB are fed as the input latent vectors to the next, i.e.,  $IEMB \leftarrow OEMB$ . Similar in style to that of iterative attention, the value of  $IEMB$  of the first stacked CMAB block is learned.

CMAB initially compresses the input data by applying a cross-attention between the input data and a fixed set of  $L_B$  latents  $BEMB$  whose value is learned during training. Next, self-attention is used to compute higher-order information:

$$DEMB = \text{SelfAttention}(\text{CrossAttention}(BEMB, INPUT))$$

Afterwards, another cross-attention between the input vectors  $IEMB$  and  $DEMB$  is performed and an additional self-attention is used to further compute higher-order information, resulting in the output vectors  $OEMB$ :

$$OEMB = \text{SelfAttention}(\text{CrossAttention}(IEMB, DEMB))$$

In summary, CMAB works as follows:

$$\text{CMAB}(IEMB, INPUT) = \text{SA}(\text{CA}(IEMB, \text{SA}(\text{CA}(BEMB, INPUT))))$$

where  $\text{SA}$  represents SelfAttention and  $\text{CA}$  represents CrossAttention. The two cross-attentions have a linear complexity of  $O(NL_B)$  and a constant complexity  $O(L_B L_I)$ , respectively. The self-attentions have constant complexities of  $O(L_B^2)$  and  $O(L_I^2)$ , respectively. As such, the total computation required to compute the output of the block is  $O(NL_B + L_B^2 + L_B L_I + L_I^2)$  where  $L_B$  and  $L_I$  are hyperparameter constants which bottleneck the amount of information which can be encoded.

**Constant Computation Updates.** A significant advantage of CMABs is that when given new<sup>1</sup> inputs, CMAB can compute the updated output in constant computation per new datapoint. In

<sup>1</sup>CMABs also allow for efficient removal of datapoints (and consequently edits as well) to the input data, but this is outside the scope of this work.

contrast, a transformer block would require re-computing its output from scratch, requiring quadratic computation to perform a similar update.

Having computed  $\text{CMAB}(\text{IEMB}, \text{INPUT})$  and given new datapoints  $\mathcal{D}_U$  (e.g., from sequential settings such as contextual bandits),  $\text{CMAB}(\text{IEMB}, \text{INPUT} \cup \mathcal{D}_U)$  can be computed in  $O(|\mathcal{D}_U|)$ , i.e., a constant amount of computation per new datapoint.

**Proof Outline:** Since  $L_B$  and  $L_I$  are constants (hyperparameters), CMAB’s complexity is constant except for the contributing complexity part of the first attention block:  $\text{CrossAttention}(\text{BEMB}, \text{INPUT})$ , which has a complexity of  $O(NL_B)$ . As such, to achieve constant computation updates, it suffices that the updated output of this cross-attention can be updated in constant computation per datapoint. Simplified,  $\text{CrossAttention}(\text{BEMB}, \text{INPUT})$  is computed as follows:

$$\text{CrossAttention}(\text{BEMB}, \text{INPUT}) = \text{softmax}(QK^T)V$$

where  $K$  and  $V$  are key, value matrices respectively that represent the embeddings of  $\text{INPUT}$  and  $Q$  is the query matrix representing the embeddings of  $\text{BEMB}$ . When an update with  $\mathcal{D}_U$  new datapoints occurs,  $|\mathcal{D}_U|$  rows are added to the key, value matrices. However, the query matrix is constant due to  $\text{BEMB}$  being a fixed set of latent vectors whose values are learned. As a result, the output of the cross-attention can be computed via a rolling average in  $O(|\mathcal{D}_U|)$ . A formal proof and description of this process is included in the Appendix.

As a result, we have the following property of the update function:

$$\text{CrossAttention}(\text{BEMB}, \text{INPUT} \cup \mathcal{D}_U) = \text{UPDATE}(\mathcal{D}_U, \text{CrossAttention}(\text{BEMB}, \text{INPUT}))$$

where the  $\text{UPDATE}$  operation has a complexity of  $O(|\mathcal{D}_U|)$ . Each of the remaining self-attention and cross-attention blocks only requires constant computation. As such, CMAB can compute its updated output in  $O(|\mathcal{D}_U|)$ , i.e., a constant amount of computation per datapoint.

**Computing Output in Constant Memory.** Interestingly, CMABs can compute its output in constant memory regardless of the number of inputs. Naively computing the output of CMAB is non-constant memory due to  $\text{CrossAttention}(\text{BEMB}, \text{CONTEXT})$  having a linear memory complexity of  $O(NL_B)$ . To achieve constant memory computation, we split the input data  $\text{INPUT}$  into  $N/B_C$  batches of input datapoints of size up to  $B_C$  (a pre-specified constant), i.e.,  $\text{INPUT} = \cup_{i=1}^{N/B_C} \mathcal{D}_i$ . Instead of computing the output at once, it is equivalent to performing the update  $N/B_C - 1$  times:

$$\text{CA}(\text{BEMB}, \text{INPUT}) = \text{UPD}(\mathcal{D}_1, \text{UPD}(\mathcal{D}_2, \dots \text{UPD}(\mathcal{D}_{N/B_C-1}, \text{CA}(\text{BEMB}, \mathcal{D}_{N/B_C}))))$$

where  $\text{UPD}$  is an abbreviation for  $\text{UPDATE}$ . Computing  $\text{CrossAttention}(\text{BEMB}, \mathcal{D}_{N/B_C})$  requires  $O(L_B B_C)$  constant memory. After its computation, the memory can be freed up, so that each of the subsequent  $\text{UPDATE}$  operations can re-use the memory space. Each of the update operations cost  $O(L_B B_C)$  constant memory, resulting in  $\text{CrossAttention}(\text{BEMB}, \text{INPUT})$  only needing constant memory  $O(L_B B_C)$ . As a result, CMAB’s output can be computed in constant memory.

CMABs are generally useful in that they are a more efficient alternative to transformer or iterative attention in many settings. In this work, we show their effectiveness for Neural Processes. In the Appendix, we show their effectiveness for Temporal Point Processes by replacing the transformer encoder with a CMAB-based encoder. A further advantage of CMABs over prior attention works is that the original input data does not need to be stored when performing updates, meaning the model has privacy-preserving properties and is applicable to streaming data settings (e.g., settings where the data is not stored).

### 3.2 Constant Memory Attentive Neural Processes (CMANP)

In this section, we leverage CMAB to construct an efficient Neural Process. CMANPs (Figure 2) comprise of stacked CMAB blocks which take as input the context dataset. The conditioning, querying, and updating phases in CMANPs work as follows:

**Conditioning Phase:** In the conditioning phase, the CMAB blocks encode the context dataset into a constant number of latent vectors  $\text{LEMB}_i$ . The first block takes as input a set of meta-learned latent vectors  $\text{LEMB}_0$  (i.e.,  $\text{IEMB}$  in CMABs) and the context dataset  $\text{CONTEXT}$  and outputs a set of

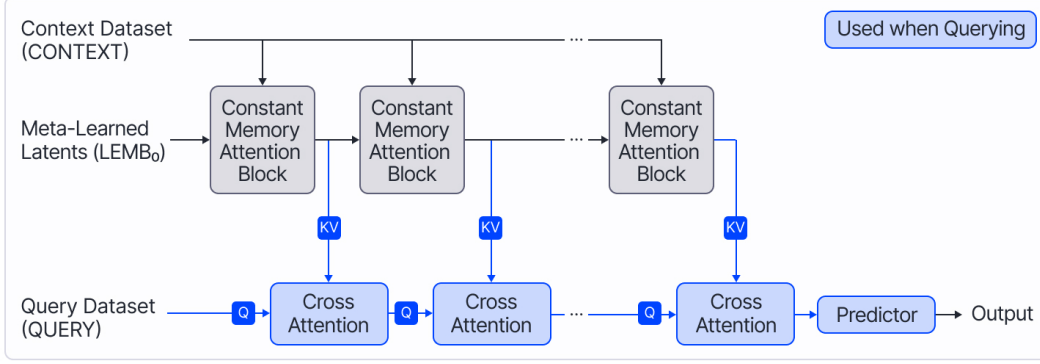


Figure 2: Constant Memory Attentive Neural Processes

encodings  $LEMB_1$  (i.e., OEMB in CMABs). The output latents of each block are passed as the input latents to the next CMAB block.

$$LEMB_i = \text{CMAB}(LEMB_{i-1}, \text{CONTEXT})$$

Since CMAB can compute its output in constant memory, thus CMANPs can also perform this conditioning phase in constant memory.

**Querying Phase:** In the querying phase, the deployed model retrieves information from the fixed size outputs of the CMAB blocks ( $LEMB_i$ ) to make predictions for the query dataset (QUERY). When making a prediction for query datapoints, information is retrieved via cross-attention.

$$\begin{aligned} QEMB_0 &= \text{QUERY} \\ QEMB_i &= \text{CrossAttention}(QEMB_{i-1}, LEMB_i) \\ \text{Output} &= \text{Predictor}(QEMB_K) \end{aligned}$$

**Update Phase:** In the update phase, the NP receives a batch of new datapoints  $\mathcal{D}_U$  to include in the context dataset. CMANPs leverage the efficient update mechanism of CMABs to achieve efficient updates (constant per datapoint) to its context dataset. Specifically, the first CMAB block updates its output using the new datapoints. Afterwards, the next CMAB blocks are updated sequentially using the updated output of the previous CMAB block as follows:

$$\begin{aligned} LEMB'_0 &= LEMB_0 \\ LEMB'_i &= \text{CMAB}(LEMB'_{i-1}, \text{CONTEXT} \cup \mathcal{D}_U) \end{aligned}$$

Since CMAB can compute the output and perform updates in constant memory irrespective of the number of context datapoints, CMANPs can also compute its output and perform the update in constant memory. In Table 1, we compare the memory complexities of top-performing Neural Processes, showcasing the efficiency gains of CMANP over prior state-of-the-art methods.

### 3.2.1 Autoregressive Not-Diagonal

In many settings where NPs are applied such as Image Completion, the target datapoints are correlated and its predictive distribution are evaluated altogether. As such, prior works (Nguyen and Grover, 2022; Feng et al., 2023) have proposed a Not-Diagonal variant of NPs which predict the mean and a full covariance matrix, typically via a low-rank approximation. This is in contrast from the vanilla (Diagonal) variants which predict the mean and a diagonal covariance matrix. Not-Diagonal methods, however, are not scalable due to outputting a full covariance matrix is quadratic in the number of target datapoints, requiring at least quadratic memory.

Leveraging the efficient updates property of CMABs, we propose CMANP-AND (Autoregressive Not Diagonal). During training, CMANP-AND is trained as a Not-Diagonal variant, i.e., maximising the likelihood. When deployed, the model is treated as an autoregressive model that makes predictions in blocks of size  $B_Q$  datapoints. For each block prediction, a mean and full covariance matrix is computed via a low-rank approximation. Sampled predictions of prior blocks are used to make

	Memory Complexity				
	Conditioning	Querying		Updating	
In Terms of	$N$	$N$	$M$	$N$	$ \mathcal{D}_U $
TNP-D	N/A	✗	✗	N/A	N/A
TNP-ND	N/A	✗	✗	N/A	N/A
EQTNP	✗	✗	✗	✗	✗
LBANP	✗	✓	✗	✗	✗
LBANP-ND	✗	✓	✗	✗	✗
CMANP (Ours)	✓	✓	✗	✓	✓
CMANP-AND (Ours)	✓	✓	✗	✓	✓

Table 1: Comparison of Memory Complexities of top-performing Neural Processes with respect to the number of context datapoints  $N$ , number of target datapoints in a batch  $M$ , and a set of new datapoints in an update  $\mathcal{D}_U$ . (Green) Checkmarks represent requiring constant memory, (Orange) half checkmarks represent requiring linear memory, and (Red) Xs represent requiring quadratic or more memory.

predictions for later blocks. Specifically, the predictions are added as new context datapoints via CMANP’s efficient update mechanism for predictions of the next block:

$$p_{\theta}(y_{N+kB_Q+1:N+(k+1)B_Q} | \hat{D}_k, x_{N+kB_Q+1:N+(k+1)B_Q}) = \mathcal{N}(\mu_{\theta}(\hat{D}_k, x_{N+kB_Q+1:N+(k+1)B_Q}), \Sigma_{\theta}(\hat{D}_k, x_{N+kB_Q+1:N+(k+1)B_Q}))$$

where  $\hat{D}_k = \{(x_i, y_i)\}_{i=1}^N \cup \{(x_i, \hat{y}_i)\}_{i=N+1}^{N+kB_Q}$  and  $k$  is the number of blocks already processed. In this setting,  $\{(x_i, y_i)\}_{i=1}^N$  refers to the original context datapoints.  $\{(x_i, \hat{y}_i)\}_{i=N+1}^{N+kB_Q}$  refers to the sampled predictions of prior blocks.  $B_Q$  is a hyperparameter which controls (1) the computational cost of the model in terms of memory and sequential computation length and (2) the performance of the model. Lower values of  $B_Q$  offer better performance but require more forward passes of the model, thus requiring more time. Since  $B_Q$  is a constant, this model makes predictions in constant memory unlike prior Not-Diagonal variants which were quadratic in memory. Crucially, this means that unlike prior Not-Diagonal variants, the model is not bottlenecked by its memory requirement, allowing for CMANP-AND to scale to larger number of datapoints than prior methods.

**Complexity Analysis:** For a batch of  $M$  datapoints and a prediction block size of  $B_Q$  (hyperparameter constant), there are  $\lceil \frac{M}{B_Q} \rceil$  batches of datapoints whose predictions are made autoregressively. Each batch incurs a constant complexity of  $O(B_Q)^2$  due to predicting a full covariance matrix. As such for a batch of  $M$  target datapoints, CMANP-AND requires a sub-quadratic total computation of  $O(\lceil \frac{M}{B_Q} \rceil B_Q^2) = O(MB_Q)$  with a sequential computation length of  $O(\frac{M}{B_Q})$ . Crucially, CMANP-AND only requires constant memory in  $N$  and linear memory in  $M$ , making it significantly more efficient than prior works which required at least quadratic memory.

**Additional Useful Properties:** In leveraging CMABs, CMANP(-AND) do not require the context dataset when updating the model, allowing for streaming data settings i.e., settings where data is not stored. As such, unlike prior work NP, the raw data would not need to be stored which is a significant advantage in settings with limited resources or where data privacy is a concern. In addition, CMANP(-AND) only requires constant memory to perform the conditioning, querying, and updating phases, making a state-of-the-art NP highly accessible for small devices.

## 4 Experiments

In this section, we evaluate CMANPs on standard NP tasks that have been extensively benchmarked: image completion and meta-regression tasks. Furthermore, we provide analysis of CMANPs, showcasing their versatility. We compare CMANPs against the large variety of members of the Neural Process family: Conditional Neural Processes (CNPs) (Garnelo et al., 2018a), Neural Processes (NPs) (Garnelo et al., 2018b), Bootstrapping Neural Processes (BNPs) (Lee et al., 2020), (Conditional) Attentive Neural Processes (C)ANPs (Kim et al., 2019), and Bootstrapping Attentive Neural Processes (BANPs) (Lee et al., 2020). In addition, we compare against the recent state-of-the-art methods:

Latent Bottlenecked Attentive Neural Processes (LBANPs) (Feng et al., 2023) and Transformer Neural Processes (TNPs) (Nguyen and Grover, 2022). We also compare against the Not-Diagonal variants of the state-of-the-art methods (LBANP-ND and TNP-ND).

For the purpose of consistency, we set the number of latents (i.e., bottleneck size)  $L_I = L_B = 128$  across all experiments. We also set  $B_Q = 5$ . Similarly, for LBANPs, we report results with the number of latents (i.e., bottleneck size)  $L = 128$  across all experiments. We show in the analysis section that our reported performance of CMANPs can be further improved by increasing the number of latents ( $L_I$  or  $L_B$ ) and decreasing the prediction block size  $B_Q$ .

Due to space limitations, several details are included in the appendix (1) experiments on contextual multi-armed bandits (2) implementation details<sup>2</sup> such as hyperparameters and their selection are included in the Appendix (3) an application of CMABs on Temporal Point Processes, showing their general applicability.

#### 4.1 Image Completion

In this setting, we consider the image completion setting with two datasets: EMNIST (Cohen et al., 2017) and CelebA (Liu et al., 2015). The model is given a set of pixel values of an image and aims to predict the remaining pixels of the image. Each image corresponds to a unique function (Garnelo et al., 2018b). In this experiment, the  $x$  values are rescaled to  $[-1, 1]$  and the  $y$  values are rescaled to  $[-0.5, 0.5]$ . For each task, a randomly selected set of pixels are selected as context datapoints and target datapoints.

EMNIST comprises of black and white images of handwritten letters of  $32 \times 32$  resolution. 10 classes are used for training. The context and target datapoints are sampled according to  $N \sim \mathcal{U}[3, 197]$  and  $M \sim \mathcal{U}[3, 200 - N]$  respectively. CelebA comprises of colored images of celebrity faces. Methods are evaluated on various resolutions to show scalability of the methods. In CelebA32, images are downsampled to  $32 \times 32$  and the number of context and target datapoints are sampled according to  $N \sim \mathcal{U}[3, 197]$  and  $M \sim \mathcal{U}[3, 200 - N]$  respectively. In CelebA64, the images are down-sampled to  $64 \times 64$  and  $N \sim \mathcal{U}[3, 797]$  and  $M \sim \mathcal{U}[3, 800 - N]$ . In CelebA128, the images are down-sampled to  $128 \times 128$  and  $N \sim \mathcal{U}[3, 1597]$  and  $M \sim \mathcal{U}[3, 1600 - N]$ .

**Results.** In Table 2, we compare CMANPs with existing NP baselines. Although all methods were able to be evaluated on CelebA ( $32 \times 32$ ) and EMNIST, many were not able to scale to CelebA ( $64 \times 64$ ) and CelebA ( $128 \times 128$ ). And all Not-Diagonal variants were not able to be trained on CelebA ( $64 \times 64$ ) and CelebA ( $128 \times 128$ ) due to being too computationally expensive, requiring quadratic computation and memory. In contrast, CMANP(-AND) was not affected by this limitation. The results show that CMANP-AND achieves clear state-of-the-art results on CelebA ( $32 \times 32$ ), CelebA ( $64 \times 64$ ), and CelebA ( $128 \times 128$ ). Furthermore, CMANP-AND achieves results competitive with state-of-the-art on EMNIST.

#### 4.2 1-D Regression

In this experiment, the model aims to model an unknown function  $f$  and make predictions for a batch of  $M$  target datapoints given a batch of  $N$  context datapoints. During each training epoch, a batch of  $B = 16$  functions are sampled from a GP prior with an RBF kernel  $f_i \sim GP(m, k)$  where  $m(x) = 0$  and  $k(x, x') = \sigma_f^2 \exp(-\frac{(x-x')^2}{2l^2})$ . The hyperparameters are sampled according to  $l \sim \mathcal{U}[0.6, 1.0]$ ,  $\sigma_f \sim \mathcal{U}[0.1, 1.0]$ ,  $N \sim \mathcal{U}[3, 47]$ , and  $M \sim \mathcal{U}[3, 50 - N]$ . After training, the models are evaluated according to the log-likelihood of the targets on functions sampled from GPs with RBF and Matern  $5/2$  kernels.

**Results.** As shown in Table 3, CMANP-AND outperforms all baselines except for TNP-ND by a significant margin. CMANP-AND achieves comparable results to TNP-ND while only requiring constant memory.

##### 4.2.1 Analysis

In our analyses, we consider CMANP models that were trained on CelebA ( $64 \times 64$ ).

---

<sup>2</sup>The code will be released upon acceptance.

Method	CelebA			EMNIST	
	32x32	64x64	128x128	Seen (0-9)	Unseen (10-46)
CNP	$2.15 \pm 0.01$	$2.43 \pm 0.00$	$2.55 \pm 0.02$	$0.73 \pm 0.00$	$0.49 \pm 0.01$
CANP	$2.66 \pm 0.01$	$3.15 \pm 0.00$	—	$0.94 \pm 0.01$	$0.82 \pm 0.01$
NP	$2.48 \pm 0.02$	$2.60 \pm 0.01$	$2.67 \pm 0.01$	$0.79 \pm 0.01$	$0.59 \pm 0.01$
ANP	$2.90 \pm 0.00$	—	—	$0.98 \pm 0.00$	$0.89 \pm 0.00$
BNP	$2.76 \pm 0.01$	$2.97 \pm 0.00$	—	$0.88 \pm 0.01$	$0.73 \pm 0.01$
BANP	$3.09 \pm 0.00$	—	—	$1.01 \pm 0.00$	$0.94 \pm 0.00$
TNP-D	$3.89 \pm 0.01$	$5.41 \pm 0.01$	—	<b><math>1.46 \pm 0.01</math></b>	<b><math>1.31 \pm 0.00</math></b>
LBANP	$3.97 \pm 0.02$	$5.09 \pm 0.02$	$5.84 \pm 0.01$	$1.39 \pm 0.01$	$1.17 \pm 0.01$
CMANP (Ours)	$3.93 \pm 0.05$	$5.02 \pm 0.14$	$5.55 \pm 0.01$	$1.36 \pm 0.01$	$1.09 \pm 0.01$
TNP-ND	$5.48 \pm 0.02$	—	—	<b><math>1.50 \pm 0.00</math></b>	<b><math>1.31 \pm 0.00</math></b>
LBANP-ND	$5.57 \pm 0.03$	—	—	$1.42 \pm 0.01$	$1.14 \pm 0.01$
CMANP-AND (Ours)	<b><math>6.31 \pm 0.04</math></b>	<b><math>6.96 \pm 0.07</math></b>	<b><math>7.15 \pm 0.14</math></b>	<b><math>1.48 \pm 0.03</math></b>	$1.19 \pm 0.03$

Table 2: Image Completion Experiments. Each method is evaluated with 5 different seeds according to the log-likelihood (higher is better). The "dash" represents methods that could not be run because of the large memory requirement.

**Empirical Memory:** In Figure 3, we compare the empirical memory cost of the various state-of-the-art NP methods during evaluation. Comparing the vanilla variants of NPs, we see that TNP-D scales quadratically with respect to the number of context datapoints while LBANP scales linearly. In contrast, CMANPs only require a low constant amount of memory regardless of the number of context datapoints. Comparing the Not-Diagonal variant of NPs, we see that both TNP-ND and LBANP-ND scale quadratically with respect to the number of target datapoints, limiting their applications. In contrast, CMANP-AND can scale to far larger number of target datapoints. As a result of our experiments, we can note that CMANPs compared with prior methods are (1) significantly more efficient (2) more scalable and (3) achieves state-of-the-art results.

Method	RBF	Matern 5/2
CNP	$0.26 \pm 0.02$	$0.04 \pm 0.02$
CANP	$0.79 \pm 0.00$	$0.62 \pm 0.00$
NP	$0.27 \pm 0.01$	$0.07 \pm 0.01$
ANP	$0.81 \pm 0.00$	$0.63 \pm 0.00$
BNP	$0.38 \pm 0.02$	$0.18 \pm 0.02$
BANP	$0.82 \pm 0.01$	$0.66 \pm 0.00$
TNP-D	$1.39 \pm 0.00$	$0.95 \pm 0.01$
LBANP	$1.27 \pm 0.02$	$0.85 \pm 0.02$
CMANP	$1.24 \pm 0.01$	$0.80 \pm 0.01$
TNP-ND	<b><math>1.46 \pm 0.00</math></b>	<b><math>1.02 \pm 0.00</math></b>
LBANP-ND	$1.24 \pm 0.03$	$0.78 \pm 0.02$
CMANP-AND	<b><math>1.48 \pm 0.03</math></b>	$0.96 \pm 0.01$

Table 3: 1-D Meta-Regression Experiments with log-likelihood metric (higher is better).

**Effect of  $B_Q$ :** In Figure 4, we compare with varying sizes of  $B_Q$  for CMANP-AND where  $B_Q$  is the size of the query block. We found that smaller block sizes achieved significantly better performance. This is expected as the autoregressive nature of the Neural Process results in a more flexible predictive distribution and hence better performance. Since the block size is inversely correlated with the required time complexity, it is recommended that when deployed CMANP-AND utilises the smallest block size for the given time limitation.

**Varying Number of Latents** In Figure 4, we evaluated the result of varying the number of input latents ( $L_I$ ) and the number of latents per block ( $L_B$ ). Empirically, we found that increasing the size of the bottleneck (i.e., number of latents  $L_I$  and  $L_B$ ) considerably improves the performance of the model. This, however, comes at a cost of increased memory requirement.

## 5 Related Work

NPs have used various methods to encode the context dataset. For example, CNPs (Garnelo et al., 2018a) encode the context set via a deep sets encoder, ConvCNPs (Gordon et al., 2019) use convolutions to build in translational equivariance. Recent work (Bruinsma et al., 2023) builds on CNPs and ConvCNPs by proposing to make them autoregressive at deployment. ANPs (Kim et al., 2019), LBANPs (Feng et al., 2023), and TNPs (Nguyen and Grover, 2022) use various kinds of attention to tackle underfitting. NP (Garnelo et al., 2018b) proposes to encode functional stochasticity in a latent variable. NPs have found a wide-range of applications which include and are not limited to Temporal



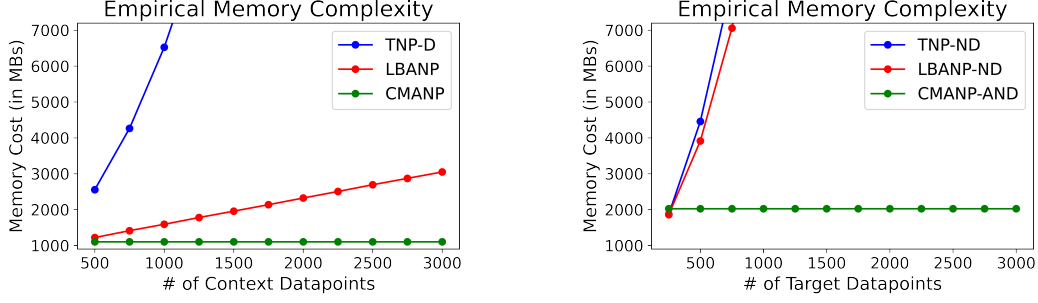


Figure 3: Memory Analyses Graphs.

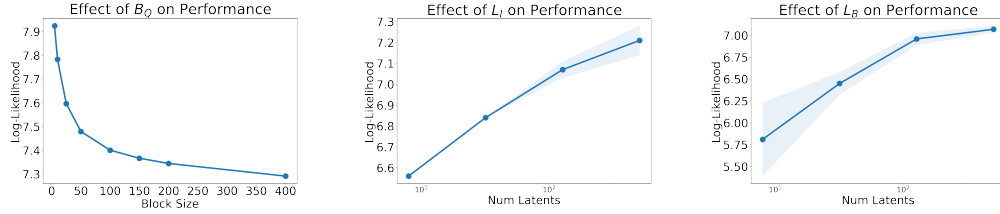


Figure 4: Analyses Graphs

Point Processes (Bae et al., 2023), sequence data (Singh et al., 2019; Willi et al., 2019), modelling stochastic physics fields (Holderrieth et al., 2021), robotics (Chen et al., 2022; Li et al., 2022), and climate modeling (Vaughan et al., 2021). For an in-depth overview, we refer the reader to the recent survey work (Jha et al., 2022) on Neural Processes and their applications.

Transformers (Vaswani et al., 2017) have achieved a large amount of success in a wide range of applications. However, the quadratic scaling of Transformers limits their applications to settings with but the quadratic scaling in terms of the number of inputs due to its self-attention layers renders it inapplicable to settings with large amounts of inputs e.g., images. There have been many proposed approaches to obtain efficiency gains such as sparse attention (Huang et al., 2019) and low-rank self-attention (Wang et al., 2020). Closest to our work, several works (Goyal et al., 2021; Jaegle et al., 2021; Lee et al., 2019) have proposed to use latent bottlenecks. Set Transformers and related works (Goyal et al., 2021; Lee et al., 2019) utilises cross-attention to map the input array back and forth between an array with fewer elements to achieve a sub-quadratic complexity. Perceiver (Jaegle et al., 2021) utilises an asymmetric cross-attention method to distill the input array into a lower-dimensional latent bottleneck; after which, standard Transformer blocks are then applied to the latent space. To the best of our knowledge, we are the first to propose an attention mechanism with an efficient update mechanism that allows for computing the output of the attention block in constant memory. For an in-depth overview, we refer the reader to the recent survey works (Khan et al., 2022; Lin et al., 2022) on Transformers and their applications.

## 6 Conclusion

In this work, we introduced CMAB (Constant Memory Attention Block), a novel efficient attention block capable of computing its output in **constant** additional memory. Building on CMAB, we proposed Constant Memory Attentive Neural Processes (CMANPs), a new NP variant requiring only constant memory for all 3 phases of Neural Processes (conditioning, querying, and updating). Leveraging the efficient updates property of CMAB, we introduced CMANP-AND (Autoregressive Not-Diagonal). Our experiments show that CMANP(-AND) achieves state-of-the-art results while being more scalable than prior methods. In our analysis, we showed that either by increasing the size of the latent bottleneck ( $L_I$  and  $L_B$ ) or decreasing the block size ( $B_Q$ ), we can further improve its performance. Previous state-of-the-art NPs required memory that is linear or quadratic in the number of context datapoints; in contrast, CMANP-AND only uses constant memory in the number of context datapoints, making it applicable to settings such as low-memory domains.

## 7 Limitations

Since CMANPs use an efficient attention scheme with latent bottlenecks, it shares the limitations of similar attention methods such as works by Feng et al. (2023), Jaegle et al. (2021), Goyal et al. (2021), and Lee et al. (2019). Specifically for these attention mechanisms, if the data has high intrinsic dimensionality, a larger latent bottleneck would improve the model’s performance.

## References

- Bae, W., Ahmed, M. O., Tung, F., and Oliveira, G. L. (2023). Meta temporal point processes. In *International Conference on Learning Representations*.
- Bruinsma, W., Markou, S., Requeima, J., Foong, A. Y. K., Andersson, T., Vaughan, A., Buonomo, A., Hosking, S., and Turner, R. E. (2023). Autoregressive conditional neural processes. In *The Eleventh International Conference on Learning Representations*.
- Chen, R., Gao, N., Vien, N. A., Ziesche, H., and Neumann, G. (2022). Meta-learning regrasping strategies for physical-agnostic objects. *arXiv preprint arXiv:2205.11110*.
- Cohen, G., Afshar, S., Tapson, J., and Van Schaik, A. (2017). Emnist: Extending mnist to handwritten letters. In *2017 international joint conference on neural networks (IJCNN)*, pages 2921–2926. IEEE.
- Feng, L., Hajimirsadeghi, H., Bengio, Y., and Ahmed, M. O. (2023). Latent bottlenecked attentive neural processes. In *International Conference on Learning Representations*.
- Gal, Y. and Ghahramani, Z. (2016). Dropout as a bayesian approximation: Representing model uncertainty in deep learning. In *international conference on machine learning*, pages 1050–1059. PMLR.
- Garnelo, M., Rosenbaum, D., Maddison, C., Ramalho, T., Saxton, D., Shanahan, M., Teh, Y. W., Rezende, D., and Eslami, S. A. (2018a). Conditional neural processes. In *International Conference on Machine Learning*, pages 1704–1713. PMLR.
- Garnelo, M., Schwarz, J., Rosenbaum, D., Viola, F., Rezende, D. J., Eslami, S., and Teh, Y. W. (2018b). Neural processes. *arXiv preprint arXiv:1807.01622*.
- Gordon, J., Bruinsma, W. P., Foong, A. Y., Requeima, J., Dubois, Y., and Turner, R. E. (2019). Convolutional conditional neural processes. In *International Conference on Learning Representations*.
- Goyal, A., Didolkar, A. R., Lamb, A., Badola, K., Ke, N. R., Rahaman, N., Binas, J., Blundell, C., Mozer, M. C., and Bengio, Y. (2021). Coordination among neural modules through a shared global workspace. In *International Conference on Learning Representations*.
- Holderrieth, P., Hutchinson, M. J., and Teh, Y. W. (2021). Equivariant learning of stochastic fields: Gaussian processes and steerable conditional neural processes. In *International Conference on Machine Learning*, pages 4297–4307. PMLR.
- Huang, Z., Wang, X., Huang, L., Huang, C., Wei, Y., and Liu, W. (2019). Ccnet: Criss-cross attention for semantic segmentation. In *Proceedings of the IEEE/CVF international conference on computer vision*, pages 603–612.
- Jaegle, A., Gimeno, F., Brock, A., Vinyals, O., Zisserman, A., and Carreira, J. (2021). Perceiver: General perception with iterative attention. In *International conference on machine learning*, pages 4651–4664. PMLR.
- Jha, S., Gong, D., Wang, X., Turner, R. E., and Yao, L. (2022). The neural process family: Survey, applications and perspectives. *arXiv preprint arXiv:2209.00517*.
- Khan, S., Naseer, M., Hayat, M., Zamir, S. W., Khan, F. S., and Shah, M. (2022). Transformers in vision: A survey. *ACM computing surveys (CSUR)*, 54(10s):1–41.
- Kim, H., Mnih, A., Schwarz, J., Garnelo, M., Eslami, A., Rosenbaum, D., Vinyals, O., and Teh, Y. W. (2019). Attentive neural processes.
- Lakshminarayanan, B., Pritzel, A., and Blundell, C. (2017). Simple and scalable predictive uncertainty estimation using deep ensembles. *Advances in neural information processing systems*, 30.
- Lee, J., Lee, Y., Kim, J., Kosiorek, A., Choi, S., and Teh, Y. W. (2019). Set transformer: A framework for attention-based permutation-invariant neural networks. In *International Conference on Machine Learning*, pages 3744–3753. PMLR.

- Lee, J., Lee, Y., Kim, J., Yang, E., Hwang, S. J., and Teh, Y. W. (2020). Bootstrapping neural processes. *Advances in neural information processing systems*, 33:6606–6615.
- Li, Y., Gao, N., Ziesche, H., and Neumann, G. (2022). Category-agnostic 6d pose estimation with conditional neural processes. *arXiv preprint arXiv:2206.07162*.
- Lin, T., Wang, Y., Liu, X., and Qiu, X. (2022). A survey of transformers. *AI Open*.
- Liu, Z., Luo, P., Wang, X., and Tang, X. (2015). Deep learning face attributes in the wild. In *Proceedings of International Conference on Computer Vision (ICCV)*.
- Nguyen, T. and Grover, A. (2022). Transformer neural processes: Uncertainty-aware meta learning via sequence modeling. In *International Conference on Machine Learning*, pages 16569–16594. PMLR.
- Rastogi, R., Schiff, Y., Hacohen, A., Li, Z., Lee, I., Deng, Y., Sabuncu, M. R., and Kuleshov, V. (2023). Semi-parametric inducing point networks and neural processes. In *The Eleventh International Conference on Learning Representations*.
- Riquelme, C., Tucker, G., and Snoek, J. (2018). Deep bayesian bandits showdown: An empirical comparison of bayesian deep networks for thompson sampling. *arXiv preprint arXiv:1802.09127*.
- Shchur, O., Bilos, M., and Günnemann, S. (2020). Intensity-free learning of temporal point processes. In *International Conference on Learning Representations*.
- Singh, G., Yoon, J., Son, Y., and Ahn, S. (2019). Sequential neural processes. *Advances in Neural Information Processing Systems*, 32.
- Vaswani, A., Shazeer, N., Parmar, N., Uszkoreit, J., Jones, L., Gomez, A. N., Kaiser, Ł., and Polosukhin, I. (2017). Attention is all you need. *Advances in neural information processing systems*, 30.
- Vaughan, A., Tebbutt, W., Hosking, J. S., and Turner, R. E. (2021). Convolutional conditional neural processes for local climate downscaling. *arXiv preprint arXiv:2101.07950*.
- Wang, S., Li, B. Z., Khabsa, M., Fang, H., and Ma, H. (2020). Linformer: Self-attention with linear complexity. *arXiv preprint arXiv:2006.04768*.
- Willi, T., Masci, J., Schmidhuber, J., and Osendorfer, C. (2019). Recurrent neural processes. *arXiv preprint arXiv:1906.05915*.
- Zaheer, M., Kottur, S., Ravanbakhsh, S., Poczos, B., Salakhutdinov, R. R., and Smola, A. J. (2017). Deep sets. *Advances in neural information processing systems*, 30.
- Zuo, S., Jiang, H., Li, Z., Zhao, T., and Zha, H. (2020). Transformer hawkes process. In *International conference on machine learning*, pages 11692–11702. PMLR.

## A Appendix: Reproducibility, Implementation, and Proof Details

### A.1 Reproducibility

We use the implementation of the baselines from the official repository of TNPs (<https://github.com/tung-nd/TNP-pytorch>) and LBNPs (<https://github.com/BorealisAI/latent-bottlenecked-anp>). The datasets are standard for Neural Processes and are available in the same link. Details regarding the architecture and the implementation is included in the main paper. Additional details regarding the hyperparameters and architecture are included in the Appendix. The code will be released upon acceptance.

### A.2 CMAB’s Constant Computation Updates Proof

Recall, CMAB works as follows:

$$\text{CMAB}(\text{IEMB}, \text{INPUT}) = \text{SA}(\text{CA}(\text{IEMB}, \text{SA}(\text{CA}(\text{BEMB}, \text{INPUT}))))$$

where **SA** represents SelfAttention and **CA** represents CrossAttention. The two cross-attentions have a linear complexity of  $O(NL_B)$  and a constant complexity  $O(L_B L_I)$ , respectively. The self-attentions have constant complexities of  $O(L_B^2)$  and  $O(L_I^2)$ , respectively. As such, the total computation required to compute the output of the block is  $O(NL_B + L_B^2 + L_B L_I + L_I^2)$  where  $L_B$  and  $L_I$  are hyperparameter constants which bottleneck the amount of information which can be encoded.

Importantly, since  $L_B$  and  $L_I$  are constants (hyperparameters), CMAB’s complexity is constant except for the contributing complexity part of the first attention block:  $\text{CrossAttention}(\text{BEMB}, \text{INPUT})$ , which has a complexity of  $O(NL_B)$ . To achieve constant computation updates, it suffices that the updated output of this cross-attention can be updated in constant computation per datapoint. Simplified,  $\text{CrossAttention}(\text{BEMB}, \text{INPUT})$  is computed as follows:

$$\text{emb} = \text{CrossAttention}(\text{BEMB}, \text{INPUT}) = \text{softmax}(QK^T)V$$

where  $K$  and  $V$  are key, value matrices respectively that represent the embeddings of  $\text{INPUT}$  (sets of  $N$  vectors) and  $Q$  is the query matrix representing the embeddings of  $\text{BEMB}$  (a set of  $L_B$  vectors). When an update with  $\mathcal{D}_U$  new datapoints occurs,  $|\mathcal{D}_U|$  rows are added to the key, value matrices. However, the query matrix is constant due to  $\text{BEMB}$  being a fixed set of latent vectors whose values are learned.

Without loss of generality, for simplicity, we consider the  $j$ -th output vector of the cross-attention ( $\text{emb}_j$ ). Let  $s_i = Q_{j,:}(K_{i,:})^T$  and  $v_i = V_{i,:}$ , then we have the following:

$$\text{emb}_j = \sum_{i=1}^N \frac{\exp(s_i)}{C} v_i$$

where  $C = \sum_{i=1}^N \exp(s_i)$ . Performing an update with a set of new inputs  $\mathcal{D}_U$ , results in adding  $|\mathcal{D}_U|$  rows to the  $K, V$  matrices and the following:

$$\text{emb}'_j = \sum_{i=1}^{N+|\mathcal{D}_U|} \frac{\exp(s_i)}{C'} v_i$$

where  $C' = \sum_{i=1}^{N+|\mathcal{D}_U|} \exp(s_i) = C + \sum_{i=N+1}^{N+|\mathcal{D}_U|} \exp(s_i)$ . As such, the updated embedding  $\text{emb}'_j$  can be computed via a rolling average:

$$\text{emb}'_j = \frac{C}{C'} \times \text{emb}_j + \sum_{i=N+1}^{N+|\mathcal{D}_U|} \frac{e^{s_i}}{C'} v_i$$

Computing  $\text{emb}'_j$  and  $C'$  via this rolling average only requires  $O(|\mathcal{D}_U|)$  operations when given  $C$  and  $\text{emb}$  as required. In practice, however, this is not stable. The computation can quickly run into numerical issues such as overflow problems.

**Practical Implementation:** In practice, instead of computing and storing  $C$  and  $C'$ , we instead compute and store  $\log(C)$  and  $\log(C')$ .

The update is instead computed as follows:  $\log(C') = \log(C) + \text{softplus}(T)$  where  $T = \log(\sum_{i=N+1}^{N+|\mathcal{D}_U|} \exp(s_i - \log(C)))$ .  $T$  can be computed efficiently and accurately using the log-sum-exp trick in  $O(|\mathcal{D}_U|)$ . This results in an update as follows:

$$\text{emb}'_j = \exp(\log(C) - \log(C')) \times \text{emb}_j + \sum_{i=N+1}^{N+|\mathcal{D}_U|} \exp(s_i - \log(C')) v_i$$

The resulting  $\text{emb}'$  and  $C'$  is the same. However, this method of implementation avoids the numerical issues that will occur.

**Practical Implementation (Proof):**

$$\begin{aligned} C &= \sum_{i=1}^N \exp(s_i) & C' &= \sum_{i=1}^{N+|\mathcal{D}_U|} \exp(s_i) \\ \log(C') - \log(C) &= \log\left(\sum_{i=1}^{N+|\mathcal{D}_U|} \exp(s_i)\right) - \log\left(\sum_{i=1}^N \exp(s_i)\right) \\ \log(C') &= \log(C) + \log\left(\frac{\sum_{i=1}^{N+|\mathcal{D}_U|} \exp(s_i)}{\sum_{i=1}^N \exp(s_i)}\right) \\ \log(C') &= \log(C) + \log\left(1 + \frac{\sum_{i=N+1}^{N+|\mathcal{D}_U|} \exp(s_i)}{\sum_{i=1}^N \exp(s_i)}\right) \\ \log(C') &= \log(C) + \log\left(1 + \frac{\sum_{i=N+1}^{N+|\mathcal{D}_U|} \exp(s_i)}{\exp(\log(C))}\right) \\ \log(C') &= \log(C) + \log\left(1 + \sum_{i=N+1}^{N+|\mathcal{D}_U|} \exp(s_i - \log(C))\right) \end{aligned}$$

Let  $T = \log(\sum_{i=N+1}^{N+|\mathcal{D}_U|} \exp(s_i - \log(C)))$ . Note that  $T$  can be computed efficiently using the log-sum-exp trick in  $O(|\mathcal{D}_U|)$ . Also, recall the softplus function is defined as follows:  $\text{softplus}(T) = \log(1 + \exp(T))$ . As such, we have the following:

$$\begin{aligned} \log(C') &= \log(C) + \log(1 + \exp(T)) \\ &= \log(C) + \text{softplus}(T) \end{aligned}$$

Recall:

$$\text{emb}'_j = \frac{C}{C'} \times \text{emb}_j + \sum_{i=N+1}^{N+|\mathcal{D}_U|} \frac{\exp(s_i)}{C'} v_i$$

Re-formulating it using  $\log(C)$  and  $\log(C')$  instead of  $C$  and  $C'$  we have the following update:

$$\text{emb}'_j = \exp(\log(C) - \log(C')) \times \text{emb}_j + \sum_{i=N+1}^{N+|\mathcal{D}_U|} \exp(s_i - \log(C')) v_i$$

which only requires  $O(|\mathcal{D}_U|)$  computation (i.e., constant computation per datapoint) while avoiding numerical issues.

### A.3 Additional Properties

In this section, we show that CMANPs uphold the context and target invariance properties.

**Property: Context Invariance.** A Neural Process  $p_\theta$  is context invariant if for any choice of permutation function  $\pi$ , context datapoints  $\{(x_i, y_i)\}_{i=1}^N$ , and target datapoints  $x_{N+1:N+M}$ ,

$$p_\theta(y_{N+1:N+M} | x_{N+1:N+M}, x_{1:N}, y_{1:N}) = p_\theta(y_{N+1:N+M} | x_{N+1:N+M}, x_{\pi(1):\pi(N)}, y_{\pi(1):\pi(N)})$$

**Proof Outline:** Since CMANPs retrieve information from a compressed encoding of the context dataset computed by CMAB (Constant Memory Attention Block). It suffices to show that CMABs compute their output while being order invariant in their input (i.e., context dataset in CMANPs (INPUT)).

Recall CMAB’s work as follows:

$$\text{CMAB}(\text{IEMB}, \text{INPUT}) = \text{SA}(\text{CA}(\text{IEMB}, \text{SA}(\text{CA}(\text{BEMB}, \text{INPUT}))))$$

where IEMB are a set of vectors outputted by prior blocks, BEMB are a set of vectors whose values are learned during training, and INPUT are the set of inputs in which we wish to be order invariant in.

The first cross-attention to be computed is:  $\text{CA}(\text{BEMB}, \text{INPUT})$ . A nice feature of cross-attention is that its order invariant in the keys and values; in this case, these are embeddings of INPUT. In other words, the output of  $\text{CA}(\text{BEMB}, \text{INPUT})$  is order invariant in the input data INPUT.

Since the remaining self-attention and cross-attention blocks take as input: IEMB and the output of  $\text{CA}(\text{BEMB}, \text{INPUT})$ , both of which are order invariant in INPUT, therefore the output of CMAB is order invariant in INPUT.

As such, CMANPs are also context invariant as required.

**Property: Target Equivariance.** A model  $p_\theta$  is target equivariant if for any choice of permutation function  $\pi$ , context datapoints  $\{(x_i, y_i)\}_{i=1}^N$ , and target datapoints  $x_{N+1:N+M}$ ,

$$p_\theta(y_{N+1:N+M} | x_{N+1:N+M}, x_{1:N}, y_{1:N}) = p_\theta(y_{\pi(N+1):\pi(N+M)} | x_{\pi(N+1):\pi(N+M)}, x_{1:N}, y_{1:N})$$

**Proof Outline:** The vanilla variant of CMANPs makes predictions similar to that of LBANPs (Feng et al., 2023) by retrieving information from a set of latent vectors via cross-attention and uses an MLP (Predictor). The architecture design ensures that the result is equivalent to making the predictions independently. As such, CMANPs preserve target equivariance the same way LBANPs do.

However, for the Autoregressive Not-Diagonal variant (CMANP-AND), the target equivariance is not held as it depends on the order in which the datapoints are processed. This is in common with that of prior methods by Nguyen and Grover (2022) and Bruinsma et al. (2023).

#### A.4 Implementation and Hyperparameter Details

We follow closely the hyperparameters of TNPs and LBANPs. In CMANP, the number of blocks for the conditioning phase is equivalent to the number of blocks in the conditioning phase of LBANP. Similarly, the number of cross-attention blocks for the querying phase is equivalent to that of LBANP. We used an ADAM optimizer with a standard learning rate of  $5e - 4$ . We performed a grid-search over the weight decay term  $\{0.0, 0.00001, 0.0001, 0.001\}$ . Consistent with prior work (Feng et al., 2023) who set their number of latents  $L = 128$ , we also set the number of latents to the same fixed value  $L_I = L_B = 128$  without tuning. Due to CMANPs and CMABs architecture, they allow for varying embedding sizes for the learned latent values (LEMB<sub>0</sub> and BEMB). For simplicity, we set the embedding sizes to 64 consistent with prior works (Nguyen and Grover, 2022; Feng et al., 2023). The block size for CMANP-AND is set as  $B_Q = 5$ . During training, CelebA (128x128), (64x64), and (32x32) used a mini-batch size of 25, 50, and 100 respectively. All experiments are run with 5 seeds. For the Autoregressive Not-Diagonal experiments, we follow TNP-ND and LBANP-ND (Nguyen and Grover, 2022; Feng et al., 2023) and use cholesky decomposition for our LBANP-AND experiments. All experiments were either run on a GTX 1080ti (12 GB RAM) or P100 GPU (16 GB RAM).

#### A.5 Compute

We trained CMANP(-AND) on a mix of Nvidia 1080Ti and P100 gpus. 1-D regression experiments took 4 hours to train. EMNIST took 2 hours to train. CelebA (32x32) took 16 hours to train. CelebA (64x64) took 2 days to train. CelebA (128x128) took 3 days to train.

	Mooc			Reddit		
	RMSE	NLL	ACC	RMSE	NLL	ACC
THP	$0.202 \pm 0.017$	$0.267 \pm 0.164$	$0.336 \pm 0.007$	$0.238 \pm 0.028$	$0.268 \pm 0.098$	$0.610 \pm 0.002$
CMHP	$0.168 \pm 0.011$	$-0.040 \pm 0.620$	$0.237 \pm 0.024$	$0.262 \pm 0.037$	$0.528 \pm 0.209$	$0.609 \pm 0.003$

Table 4: Temporal Point Processes Experiments.

## B Appendix: Additional Experiments and Analyses

### B.1 Additional CMABs application: Temporal Point Processes (TPPs)

In this section, we highlight the effectiveness of our proposed Constant Memory Attention Block by applying it to settings beyond that of Neural Processes. Specifically, we apply CMABs to Temporal Point Processes (TPPs). In brief, Temporal Point Processes are stochastic processes composed of a time series of discrete events. Recent works have proposed to model this via a neural network. Notably, models such as THP (Zuo et al., 2020) encode the history of past events to predict the next event, i.e., modelling the predictive distribution of the next event  $p_{\theta}(\tau_{l+1}|\tau_{\leq l})$  where  $\theta$  are the parameters of the model,  $\tau$  represents an event, and  $l$  is the number of events that have passed. Typically, an event comprises a discrete temporal (time) stamp and a mark (categorical class).

#### B.1.1 Constant Memory Hawkes Processes (CMHPs)

Building on CMABs, we introduce the Constant Memory Hawkes Process (CMHPs), a model which replaced the transformer layers in Transformer Hawkes Process (THP) (Zuo et al., 2020) with Constant Memory Attention Blocks. However, unlike THPs which summarise the information for prediction in a single vector, CMHPs summarise it into a set of latent vectors. As such, a flatten operation is added at the end of the model. Following prior work (Bae et al., 2023; Shchur et al., 2020), we use a mixture of log-normal distribution as the decoder for both THP and CMHP.

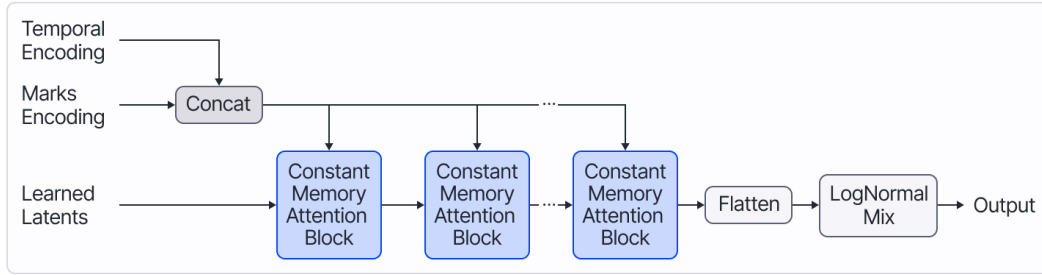


Figure 5: Constant Memory Hawkes Processes

#### B.1.2 CMHPs: Experiments

In this experiment, we compare CMHPs against THPs on standard TPP datasets: Mooc and Reddit.

**Mooc Dataset.** comprises of 7,047 sequences. Each sequence contains the action times of an individual user of an online Mooc course with 98 categories for the marks.

**Reddit Dataset.** comprises of 10,000 sequences. Each sequence contains the action times from the most active users with marks being one of the 984 the sub-reddit categories of each sequence.

The results (Table 4) suggest that replacing the transformer layer with CMAB (Constant Memory Attention Block) results in a small drop in performance. Crucially, unlike THP, CMHP has the ability to efficiently update the model with new data as it arrives overtime which is typical in time series data such as in Temporal Point Processes. CMHP only pays constant computation to update the model unlike the quadratic computation required by THP.



Method	$\delta = 0.7$	$\delta = 0.9$	$\delta = 0.95$	$\delta = 0.99$	$\delta = 0.995$
Uniform	$100.00 \pm 1.18$	$100.00 \pm 3.03$	$100.00 \pm 4.16$	$100.00 \pm 7.52$	$100.00 \pm 8.11$
CNP	$4.08 \pm 0.29$	$8.14 \pm 0.33$	$8.01 \pm 0.40$	$26.78 \pm 0.85$	$38.25 \pm 1.01$
CANP	$8.08 \pm 9.93$	$11.69 \pm 11.96$	$24.49 \pm 13.25$	$47.33 \pm 20.49$	$49.59 \pm 17.87$
NP	$1.56 \pm 0.13$	$2.96 \pm 0.28$	$4.24 \pm 0.22$	$18.00 \pm 0.42$	$25.53 \pm 0.18$
ANP	$1.62 \pm 0.16$	$4.05 \pm 0.31$	$5.39 \pm 0.50$	$19.57 \pm 0.67$	$27.65 \pm 0.95$
BNP	$62.51 \pm 1.07$	$57.49 \pm 2.13$	$58.22 \pm 2.27$	$58.91 \pm 3.77$	$62.50 \pm 4.85$
BANP	$4.23 \pm 16.58$	$12.42 \pm 29.58$	$31.10 \pm 36.10$	$52.59 \pm 18.11$	$49.55 \pm 14.52$
TNP-D	<b><math>1.18 \pm 0.94</math></b>	<b><math>1.70 \pm 0.41</math></b>	$2.55 \pm 0.43$	<b><math>3.57 \pm 1.22</math></b>	<b><math>4.68 \pm 1.09</math></b>
LBANP	<b><math>1.11 \pm 0.36</math></b>	<b><math>1.75 \pm 0.22</math></b>	<b><math>1.65 \pm 0.23</math></b>	$6.13 \pm 0.44$	$8.76 \pm 0.15$
CMANP (Ours)	<b><math>0.93 \pm 0.12</math></b>	<b><math>1.56 \pm 0.10</math></b>	<b><math>1.87 \pm 0.32</math></b>	$9.04 \pm 0.42$	$13.02 \pm 0.03$

Table 5: Contextual Multi-Armed Bandit Experiments with varying  $\delta$ . Models are evaluated according to cumulative regret (lower is better). Each model is run 50 times for each value of  $\delta$ .

## B.2 Additional CMANPs Experiments: Contextual Bandits

In the Contextual Bandit setting introduced by Riquelme et al. (2018), a unit circle is divided into 5 sections which contain 1 low reward section and 4 high reward sections  $\delta$  defines the size of the low reward section while the 4 high reward sections have equal sizes. In each round, the agent has to select 1 of 5 arms that each represent one of the regions. For context during the selection, the agent is given a 2-D coordinate  $X$  and the actions it selected and rewards it received in previous rounds.

If  $\|X\| < \delta$ , then the agent is within the low reward section. If the agent pulls arm 1, then the agent receives a reward of  $r \sim \mathcal{N}(1.2, 0.012)$ . Otherwise, if the agent pulls a different arm, then it receives a reward  $r \sim \mathcal{N}(1.0, 0.012)$ . Consequently, if  $\|X\| \geq \delta$ , then the agent is within one of the four high-reward sections. If the agent is within a high reward region and selects the corresponding arm to the region, then the agent receives a large reward of  $N \sim \mathcal{N}(50.0, 0.012)$ . Alternatively, pulling arm 1 will reward the agent with a small reward of  $r \sim \mathcal{N}(1.2, 0.012)$ . Pulling any of the other 3 arms rewards the agent with an even smaller reward of  $r \sim \mathcal{N}(1.0, 0.012)$ .

During each training iteration,  $B = 8$  problems are sampled. Each problem is defined by  $\{\delta_i\}_{i=1}^B$  which are sampled according to a uniform distribution  $\delta \sim \mathcal{U}(0, 1)$ .  $N = 512$  points are sampled as context datapoints and  $M = 50$  points are sampled for evaluation. Each datapoint comprises of a tuple  $(X, r)$  where  $X$  is the coordinate and  $r$  is the reward values for the 5 arms. The objective of the model during training is to predict the reward values for the 5 arms given the coordinates (context datapoints).

During the evaluation, the model is run for 2000 steps. At each step, the agent selects the arm which maximises its UCB (Upper-Confidence Bound). After which, the agent receives the reward value corresponding to the arm. The performance of the agent is measured by the cumulative regret. For comparison, we evaluate the models with varying  $\delta$  values and report the mean and standard deviation for 50 seeds.

**Results.** In Table 5, we compare CMANPs with other NP baselines, including the recent state-of-the-art methods TNP-D, EQTNP, and LBANP. We see that CMANP achieves competitive performance with state-of-the-art for  $\delta \in \{0.7, 0.9, 0.95\}$ . However, the performance degrades as  $\delta$  reaches extreme values close to the limit such as 0.99 and 0.995 – settings that are at the edge of the training distribution.

## B.3 Additional Analyses

**Time Cost and Performance Scatterplot:** In Figure 6, we evaluate the empirical time cost of CMANP-AND with varying number of context datapoints ( $N$ ), number of target datapoints ( $M$ ), and block size ( $B_Q$ ). The number of context datapoints and number of target datapoints are shown as labels of the datapoints. The colour of the datapoint represents its respective block size. Depending on the amount of available resources (e.g., time), the value of the block size can be chosen equivalently.

**Generalisation Ability:** In Figure 7, we evaluated CMANP-AND’s potential to generalise to settings with significantly more context datapoints than originally trained on. During training, the model was trained on tasks with a maximum of 800 context datapoints. In contrast, during evaluation, we conditioned on up to 2000 context datapoints and evaluated on 800 target datapoints. Empirically, we

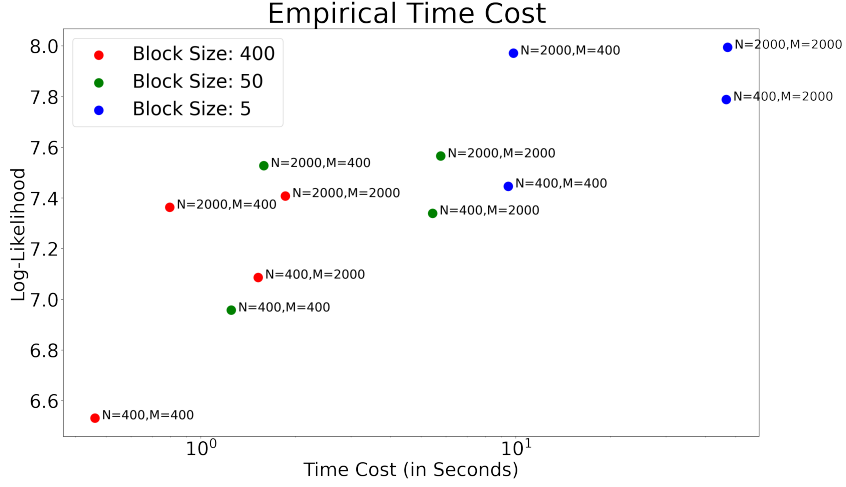


Figure 6: Scatterplot

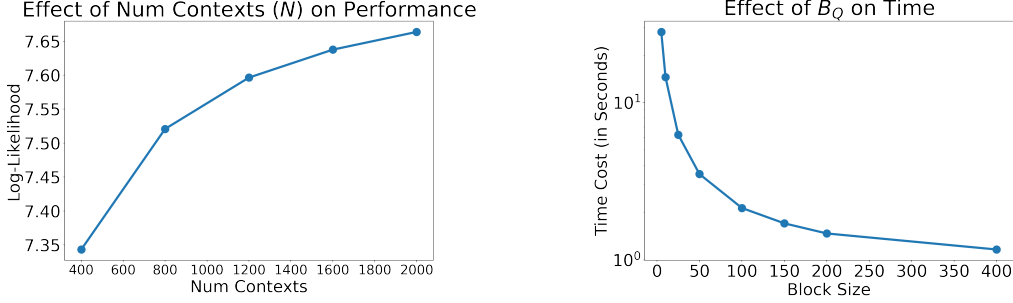


Figure 7: Additional Analyses Graphs

found that the model’s performance grows consistently as the number of context datapoints increase. However, the performance slows down at large number of contexts. We hypothesize that the cause of the saturation is due to two main factors: (1) the information gained from new context datapoints is dependent on the size of the current context dataset. For example, adding 400 new datapoints to a context dataset of size 400 results in 100% more data. Alternatively, adding 400 new datapoints to a context dataset of size 1600 results in 25% more data. As such, it is expected to see such saturation with a linear x-axis scaling. (2) in this case, CelebA (64 x 64) comprising of only 4096 pixels in total. 2000 comprises of a substantial amount of the data, i.e., approximately half. As such, saturation is expected as the amount of information gained by additional datapoints is minimal.

**Effect of Block Size ( $B_Q$ ) on Empirical Time Cost:** In Figure 7, we evaluated the time required for CMANP-AND with respect to the block size ( $B_Q$ ). The results are as expected, showing that the time required during deployment is lower as the block size increases. In the main paper, we showed that lower block sizes improve the model’s performance. In conjunction, these plots show that there is a trade-off between the time cost and performance. These results suggest that during deployment it is advisable to select smaller block sizes if allowed for the time constraint.